J. Fluid Mech. (1990), *vol.* 212, *pp.* 373–393
Printed in Great Britain

Nonlinear dynamics of two-mode interactions in parametric excitation of surface waves

By T. KAMBE AND M. UMEKI
Department of Physics, University of Tokyo, Hongo, Bunkyo-ku, Tokyo, 113, Japan

(Received 30 June 1989)

Parametric excitation of surface waves in a container under vertical forcing is investigated in detail, by an averaged Lagrangian method due to John Miles, and a system of evolution equations of third-order nonlinearity is presented for the case that the forcing frequency is chosen to be near twice the frequencies of two nearly degenerate free modes. The system of first-order differential equations in four variables which are derived from an averaged Hamiltonian is considered in a unified fashion, and the analytical results are compared with three experimental observations. It is found with the help of numerical integration that this dynamical system yields not only excitation of a single-mode state, but also interaction between two modes in which each mode oscillates either periodically or chaotically. These results are in good agreement with the observations, except for one case in which nonlinearity is considered to be too strong. As a fourth case, homoclinic chaos in the Hamiltonian system of two-degrees of freedom without damping is studied numerically. It is suggested that the chaotic mode competition observed in the experiments is different from the homoclinic chaos.

1. Introduction

Surface waves of a liquid in a container subject to vertical oscillation are being extensively investigated from the viewpoints of low-dimensional chaos in Hamiltonian systems with or without damping. In such experiments, various patterns of standing waves are observed in the free surface. Faraday (1831) and Rayleigh (1883) studied experimentally such excitation of surface waves, and noted that the frequency of the excited waves was typically one half of that of the forcing. Benjamin & Ursell (1954) showed that the linearized theory of irrotational wave motions of an inviscid fluid in a container leads to an infinite set of Mathieu equations, which allow such solutions oscillating with a subharmonic frequency. Relative to the non-inertial frame of reference fixed to the fluid container, the external forcing is equivalent to oscillation of the acceleration of gravity, and the problem is reduced to that of parametric resonance.

More recently, with a view to detecting regular, irregular or chaotic wave motions in the nonlinear resonance, Ciliberto & Gollub (1985) carried out an experiment on parametric excitation of a cylindrical fluid layer in a circular vessel. They studied excitation of a pair of non-circularly symmetric modes and found an interaction between the two modes in which the wave pattern oscillates either periodically or chaotically with a period long compared with that of the forcing. Gollub & Meyer (1983) studied a sequence of symmetry-breaking bifurcations and a discontinuous transition to a spatially disordered state. Keolian *et al.* (1981) and Keolian &

Rudnick (1984), using liquid helium and water in a thin annular trough, observed both period-doubling and quasi-periodic motion involving three modes.

Miles (1976) proposed a mathematical formulation of the weakly nonlinear problem of surface waves in a cylindrical basin, in which the Lagrangian and Hamiltonian functions for the system are constructed in terms of the generalized coordinates of the free-surface displacement. Weak dissipation is included primarily to account for friction at the container walls.

Before considering the present problem of parametric excitation of surface waves, we briefly describe how this formulation has been applied to related problems. In 1984, it was applied to the resonant response of a damped spherical pendulum to horizontal oscillation of its point of suspension (Miles 1984*a*), then to the resonant excitation of surface waves in a circular cylinder subject to horizontal or vertical forcing (Miles 1984*b*, *c*). The spherical pendulum is perhaps one of the simplest examples of a two-degrees-of-freedom oscillation with a degenerate frequency along two horizontal directions. The two degrees of freedom are uncoupled in the linear approximation, but are resonantly coupled by nonlinearity. Similar situations occur for a pair of surface wave modes of degenerate frequency ω_1 subject to a *horizontal* forcing frequency Ω in the neighbourhood of resonance ($\omega_1 \approx \Omega$, not a subharmonic resonance), the mode pair being those oscillating along two orthogonal horizontal directions in a circular cylinder of radius R.

A system of evolution equations, i.e. ordinary differential equations of third-order nonlinearity with linear damping terms (with coefficient α), has been given for a two-degrees-of-freedom system of resonant surface waves subject to horizontal forcing. The evolution equations comprise two parameters which are a damping constant α and a resonance offset $\beta = (\Omega - \omega_1)/\omega_1$. The equations reduce to the corresponding equations for either a spherical pendulum (Miles 1984*a*) or a stretched string (Miles 1984*d*) if coefficients of the nonlinear terms are fixed at certain appropriate constant values. Numerical explorations by Miles of the evolution equations for the spherical pendulum and surface waves disclosed that both of the systems exhibit a bifurcation to a steady periodic motion from a quiescent state and Hopf bifurcations to quasi-periodic motions, and further bifurcations to chaotic behaviour, under various values of the tuning parameter β. However, the response of the string appears to be regular for all α and β according to the numerical results.

Funakoshi & Inóué (1988) have performed a remarkable demonstration based on their experimental and numerical analyses on the *horizontal* excitation of surface waves in a circular container. They have shown that Miles' evolution equations predict many features of the experimental observations on the regular and chaotic wave motions, and that in particular the chaotic trajectory observed in the experiment is in fact a strange attractor, i.e. it has a positive Liapunov exponent. The observed chaotic trajectories in a phase plane are found to resemble closely those obtained from their numerical integration.

We now turn to the problem of the subharmonic resonance of surface waves in a *vertically* oscillating basin, called Faraday resonance. Based on his nonlinear evolution equations, Miles (1984*c*) found a resonant excitation of subharmonic modes of eigenfrequency ω_1 near $2\omega_1 \approx \Omega$ for the forcing frequency Ω. However, excluding the possibility of internal resonance between the eigenmodes (except for the equivalent mode obtained by an azimuthal rotation of $\frac{1}{2}\pi$), he found no Hopf bifurcations to quasi-periodic motion. Note that the system without damping is integrable. (An extension to the case of two modes in subharmonic resonance is given in Miles 1988.)

However in the presence of a 1:2 internal resonance for the two modes ($\omega_1 : \omega_2$) and in the absence of any other internal resonance, Holmes (1986) has shown mathematically that the weakly nonlinear dynamical system with forcing has transversal intersections of homoclinic orbits. This result implies that Smale horseshoes, hence sets of chaotic orbits, exist in the phase space in near resonance $2\omega_1 \approx \omega_2 \approx \Omega$. It is interesting to compare this with the analysis due to Miles (1984*c*) which shows that the exact internal resonance $2\omega_1 = \omega_2$ does not lead to Hopf bifurcation to quasi-periodic oscillation, hence not to chaotic motions. In this case of 1:2 internal resonance, the nonlinear interaction terms are of second order. For a rectangular geometry, Nayfeh (1987) and Gu & Sethna (1987) analysed the problem of interaction between modes with frequency ratio 1:2 and found chaotic behaviour. Unfortunately experimental confirmation of these predictions for the case of 1:2:2 resonance (for $\omega_1 : \omega_2 : \Omega$) remains to be done. The efforts for the rectangular case were unsuccessful, since the requirement of this frequency ratio makes the fluid height relatively small, suppressing the nonlinear phenomena due to excessive energy dissipation (Feng & Sethna 1989).

In the present paper we consider 1:1:2 resonances, i.e. $2\omega_1 \approx 2\omega_2 \approx \Omega$, in which interactions are described by the third-order nonlinear terms in the evolution equations. We shall consider three typical cases in the subsequent sections, which are studied both experimentally and analytically. Fortunately, we already have experimental evidence of chaotic mode interactions from the work of Ciliberto & Gollub (1984, 1985), as mentioned above, where surface waves in a circular cylinder of radius $R = 6.35$ cm containing water of depth $d \approx 1$ cm were observed spatially and temporally by means of digitized optical signals. They found a pair of modes interacting competitively, which are denoted as the (4, 3) and (7, 2) modes. The eigenmodes of surface deformation can be described by double-integer indices (l, m), more precisely given by the functions

$$J_l(\kappa_{lm} r)[\cos l\theta, \sin l\theta], \tag{1.1}$$

where r is the radial coordinate, θ the azimuthal coordinate, $J_l(x)$ the Bessel function of the order l, and the wavenumber κ_{lm} is determined by the boundary conditions. The linear theory due to Benjamin & Ursell (1954) predicts that the eigenfrequencies of both modes are close. From their time series data of local light intensity, Ciliberto & Gollub constructed a chaotic attractor of correlation dimension about 2.2 in the phase space, which is required to have the embedding dimension 4 to represent the time series.

Meron & Procaccia (1986*a*, *b*) derived a set of amplitude equations for comparison to this experiment, based on the centre-manifold theorem and on normal-form theory. This analysis took advantage of the experimental finding (Ciliberto & Gollub 1985) that there is a point in the parameter space where the transition to chaos occurs essentially directly from the quiescent state. This is in contrast to many other cases where the chaotic motion sets in after a series of bifurcations. However, they treated the coefficients of the third-order nonlinear terms as free parameters so as to reproduce the observed phase diagram (instead of a direct calculation).

Very recently Umeki & Kambe (1989) applied the Miles' formulation (1976, 1984*a*) to the same problem of the (4, 3) and (7, 2) mode interaction. They estimated the coefficient values of the fourth-order terms of the Hamiltonian. This is based on a fundamental principle of mechanics and leads to evolution equations for the mode amplitudes supposed to be equivalent to those of Meron & Procaccia (who neglected some nonlinear terms). The coefficients are expressed in terms of integrals of the

eigenfunctions (1.1) of the linear system and are given by a direct numerical evaluation, independently of the experiment.

In spite of this difference, the evolution equations due to Umeki & Kambe yielded phase trajectories of mode competition between (4, 3) and (7, 2), whose amplitudes have a slowly varying envelope compared to the fast oscillation at $\frac{1}{2}\Omega$, the slow variation being either periodic or chaotic. These computed motions are found in the corresponding parameter regions in the diagram of the driving frequency Ω and the amplitude a_0 as observed experimentally.

Recently, in a circular cylindrical container at the greater depth of about 5.5 cm, a different mode pair has been observed to exhibit similar competing interaction (Karatsu 1988). The new mode pair is represented as (1, 2) and (4, 1), which are lower modes oscillating at a frequency about half that of the modes (4, 3) and (7, 2). Miles' evolution equations were applied to this new pair to account for some of the experimental results.

The third case we consider is the subharmonic resonance in a square or a rectangular cylindrical container. In a recent experimental investigation of modal interactions in such geometries, helped by the analysis of the amplitude equations, Simonelli & Gollub (1989) have studied the dynamics of the interactions of two modes that are degenerate in the square layer but non-degenerate in the rectangular one owing to the symmetry breaking. They have found that the fully degenerate case yields no time-dependent envelope of amplitudes; however, in a slightly rectangular case, both periodic and chaotic interactions between the modes are observed.

On the other hand, the amplitude equations have been determined by Feng & Sethna (1989) from a perturbation analysis of the basic hydrodynamic equations. They have made a full bifurcation analysis of wave modes in a slightly rectangular cell. However, only the expected locations of the parameter values at which chaotic phenomena occur are presented together with experimental evidence of what appears to be chaotic behaviour. A bifurcation analysis was also made by Nagata (1989) for two completely degenerate modes in a square container. Crawford, Knobloch & Riecke (1988) developed a general bifurcation theory for mode interactions with symmetry and applied it to the experiment of Ciliberto & Gollub.

Recently Umeki (1989) has studied the dynamics of such systems, based on Miles' formulation, and found both periodic and chaotic trajectories in a phase space, and that the bifurcation diagram is very similar to the observations. However, in his analysis, a stable mixed standing-wave state, which has not been observed by Simonelli & Gollub, changes into a mode competition state by a subcritical Hopf bifurcation.

In the present paper we derive results from the system of nonlinear evolution equations for the surface waves, and compare them with various known results. The mathematical formulation for the surface wave problem is briefly described in §2. Analysis of stationary states of the averaged system is given in §3. Comparisons are made between experimental observations and theoretical analyses for the three cases in §4.

In §5, we consider homoclinic chaos which is represented by the present dynamical system for a different set of coefficients from those of the experimental cases. It is shown that, using a reduction method, the Hamiltonian system without forcing has homoclinic orbits, and that the presence of a small external forcing gives rise to a thin stochastic layer. However, when a small damping is added, this stochastic layer will disappear and solutions tend to a fixed point. This implies that the homoclinic

chaos in the Hamiltonian system and the chaotic mode competition observed in the strongly dissipative system are to be distinguished.

2. Mathematical formulation

In the study of nonlinear dynamics of surface waves of an inviscid incompressible irrotational fluid in a cylindrical container, three distinct methods, which should be equivalent, are normally used. Many works so far have been based on a classical perturbation method which uses two nonlinear boundary conditions at the free surface in the form of expansion with respect to the small parameter $\eta\kappa$, where η is a surface displacement and κ is a representative wavenumber. The second method relies on a canonical formulation of an average Lagrangian method due to Miles, based on a variational principle. The third one is a newly developed method by Meron & Procaccia (1986*a*, *b*) who used normal-form theory together with the centre-manifold theorem. Here we take the second approach.

In the Miles' formulation, the velocity potential ϕ and the surface displacement η are expanded as

$$\phi = \sum_n \phi_n(t)\,\psi_n(x,y)\,\operatorname{sech}\kappa_n d\,\cosh\kappa_n z, \tag{2.1}$$

$$\eta = \sum_n \eta_n(t)\,\psi_n(x,y), \tag{2.2}$$

where (x,y) and z denote the horizontal and vertical coordinates, respectively (figure 1), and the mode amplitudes $\phi_n(t)$ and $\eta_n(t)$ are related as

$$\phi_i = \sum_m l_{im}(\eta)\,\dot{\eta}_m, \tag{2.3}$$

where $l_{im}(\eta)$ is a matrix which depends on η nonlinearly. The eigenfunction ψ_n satisfies the Helmholtz equation

$$(\nabla_{\mathrm{h}}^2+\kappa_n^2)\,\psi_n = 0, \tag{2.4}$$

where $\nabla_{\mathrm{h}}^2 = \partial_x^2+\partial_y^2$, with the boundary condition for the normal derivative $\partial\psi/\partial n = 0$ on the container surface (n being the outward normal). A function $\psi_n(x,y)$ represents an eigenmode in the horizontal cross-section S, occasionally written as ψ_{mn} when the mode n is denoted by double indices (m,n).

For some simple geometrical shapes of the cross-section S, the eigenmodes are readily given. For example, for a rectangular cross-section of side lengths M by N, the mode (m,n) is given by the eigenfunction

$$\psi_{mn}(x,y) = [(2-\delta_{m0})(2-\delta_{n0})]^{\frac{1}{2}}\cos\frac{m\pi x}{M}\cos\frac{n\pi y}{N}, \tag{2.5}$$

with the wavenumber $\kappa_{mn} = [(m/M)^2+(n/N)^2]^{\frac{1}{2}}\pi$ and δ_{mn} being the Kronecker's delta.

For a circular cross-section of radius R, the eigenfunction is

$$(\psi_{mn}^{\mathrm{c}}, \psi_{mn}^{\mathrm{s}})(r,\theta) = \frac{1}{N_{mn}} J_m(\kappa_{mn} r)(\cos m\theta, \sin m\theta), \tag{2.6}$$

where $J_m(x)$ is a Bessel function of mth order, $\kappa_{mn} = j'_{mn}/R$, j'_{mn} being the nth zero of $J'_m(x)$. It should be noted that there are two completely degenerate components $(m,n)_{\mathrm{c}}$ and $(m,n)_{\mathrm{s}}$ for a circular cylinder owing to the symmetry of the shape of the

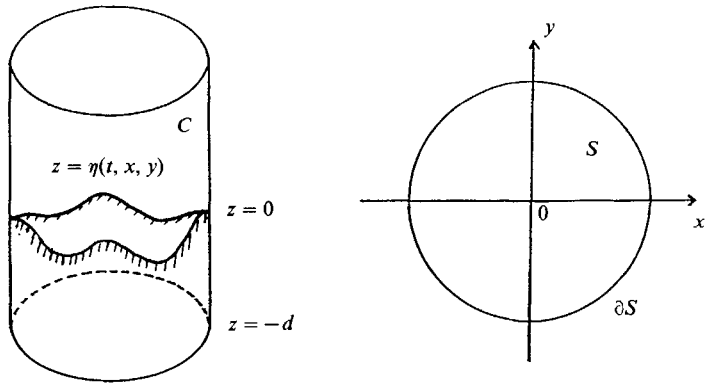

FIGURE 1. Configuration and frame of reference.

container. Similarly, the (m,n) and (n,m) modes for a square container are degenerate. Here we use the term 'component' to distinguish the completely degenerate modes.

We consider two modes (m_1, n_1) and (m_2, n_2) in subharmonic resonance, responding to the external *vertical* forcing

$$a_0 \cos \Omega t \quad \left(\omega_i = \left[\frac{g}{a_i}(1+\lambda^2\kappa_i^2)\right]^{\frac{1}{2}}, \quad i = 1, 2\right),$$

with $\Omega = 2\omega$, $\omega \approx \omega_1 \approx \omega_2$ (Ω being called the driving frequency, g the acceleration due to gravity). The displacement of the ith mode is expressed as

$$\eta_i = \epsilon a_i[p_i(\tau)\cos\omega t + q_i(\tau)\sin\omega t + \epsilon(\bar{A}_i\cos 2\omega t + \bar{B}_i \sin 2\omega t + \bar{C}_i)], \tag{2.7}$$

where $$a_i = (\kappa_i \tanh \kappa_i d)^{-1}, \quad \tau = \epsilon^2\omega t, \quad \lambda = (\gamma/\rho g)^{\frac{1}{2}}$$

and ϵ is a small parameter to be specified later; $p_i = q_i = 0$ except for $i = 1,2$ and $\bar{A}_i = \bar{B}_i = \bar{C}_i = 0$ except for the modes interacting with the resonant modes $i = 1,2$. Here p_i, q_i etc. are made dimensionless by a_i (which differs from Miles' formulation). The average Lagrangian function derived by Umeki & Kambe (1989), following Miles (1984*b*,*c*), is expressed as

$$\frac{\langle L\rangle_{\mathrm{av}}}{a^3\epsilon^4\omega^2} = \frac{1}{2}\sum_{i=1}^{2}(\dot{p}_i q_i - p_i\dot{q}_i) + H, \tag{2.8}$$

where $a = a_1\,(\approx a_2)$, and the Hamiltonian H is given by

$$H = \frac{1}{2}\sum_{i=1}^{2}[A_0(p_i^2-q_i^2) + \beta_i(p_i^2+q_i^2) + \tfrac{1}{2}A_i(p_i^2+q_i^2)^2] + \tfrac{1}{2}C(p_1^2+q_1^2)(p_2^2+q_2^2) + \tfrac{1}{2}DM^2, \tag{2.9}$$

where the forcing A_0 and the frequency offset β_i of the ith mode are normalized as

$$A_0 = a_0/a\epsilon^2, \tag{2.10}$$

$$\beta_i = (\omega^2 - \omega_i^2)/(2\epsilon^2\omega^2). \tag{2.11}$$

In (2.9) we define

$$M = p_1 q_2 - p_2 q_1, \tag{2.12}$$

$$A_1 = A, \quad A_2 = B, \tag{2.13a,b}$$

where A, B, C, D are the constant coefficients (defined in Umeki & Kambe 1989) which depend on the mode pair, the geometrical shape of the container, the depth d, the surface tension γ and the forcing frequency Ω.

The coefficients A, B, C, D and β_1, β_2 have special relations according to the symmetry and degeneracy of the boundary conditions. For example, we have (i) $A = B = C$, $\beta_1 = \beta_2$ for mode 1 given by $(m, n)_c$ and mode 2 by $(m, n)_s$ $(m \neq 0)$ in the circular container, (ii) $A = B$, $\beta_1 = \beta_2$ for mode $1 = (m, n)$ and mode $2 = (n, m)$ $(m \neq n)$ in the square container, and (iii) $A = B$ but $\beta_1 \neq \beta_2$ for (m, n) and (n, m) in the slightly rectangular container since a small difference of A and B is considered as an effect of order higher than the third nonlinearity. For two modes (m_1, n_1) and (m_2, n_2) in the circular container with different m and n values, there are no such equalities. In this case, although each mode has two completely degenerate (c, s) components, we can deal with them like a single mode. This is based on the property (Umeki & Kambe 1989) that an angular momentum associated with a pair of (c, s) components (related to a mode rotation), even if it existed initially, tends to vanish owing to the linear damping, resulting in the state of zero angular momentum of no mode rotation (or no azimuthally travelling wave state). Thus the (c, s) component pair behaves like a single mode. This feature does not hold for the horizontal forcing problem.

The dynamical equations are given by Hamilton's equations of motion with additional damping terms of a damping constant α_i:

$$\left(\frac{\mathrm{d}}{\mathrm{d}\tau}+\alpha_i\right)(p_i, q_i) = \left(-\frac{\partial}{\partial q_i}, \frac{\partial}{\partial p_i}\right)H \quad \text{for } i = 1 \text{ and } 2. \tag{2.14}$$

Writing $\bar{r}_i = p_i + \mathrm{i}q_i$ in complex notation, the evolution equations are reduced to

$$\mathrm{i}\left(\frac{\mathrm{d}}{\mathrm{d}\tau}+\alpha_1\right)\bar{r}_1 = -A_0\bar{r}_1^* - [\beta_1 + A|\bar{r}_1|^2 + (C+D)|\bar{r}_2|^2]\bar{r}_1 + D\bar{r}_1^*\bar{r}_2^2, \tag{2.15a}$$

$$\mathrm{i}\left(\frac{\mathrm{d}}{\mathrm{d}\tau}+\alpha_2\right)\bar{r}_2 = -A_0\bar{r}_2^* - [\beta_2 + B|\bar{r}_2|^2 + (C+D)|\bar{r}_1|^2]\bar{r}_2 + D\bar{r}_2^*\bar{r}_1^2, \tag{2.15b}$$

where an asterisk denotes the complex conjugate. Equilibrium states are given by the condition $\mathrm{d}/\mathrm{d}\tau = 0$. The bifurcations of those equilibrium states were considered by Feng & Sethna (1989) with the relations $A = B$, $C > A > 0$, $D < 0$ and $A + C + D > 0$. The damping constant α_i will be determined empirically such that the minimum value of the forcing, $a_{0\min}$, required to excite a single mode coincides with that of observations. We take α_i as $\alpha_1 = \alpha_2 = \alpha$ in the following analysis, although a non-zero value $\alpha_1 - \alpha_2$ is reported by Simonelli & Gollub.

3. Nonlinear evolution equations

We consider the dynamical system (2.14) or, equivalently, the two-degrees-of-freedom Hamiltonian system with linear damping terms:

$$\dot{p}_1 = -\alpha p_1 + (-\beta_1 + A_0 - Ar_1^2 - Cr_2^2)q_1 + DMp_2, \tag{3.1a}$$

$$\dot{q}_1 = -\alpha q_1 + (\beta_1 + A_0 + Ar_1^2 + Cr_2^2)p_1 + DMq_2, \tag{3.1b}$$

$$\dot{p}_2 = -\alpha p_2 + (-\beta_2 + A_0 - Br_2^2 - Cr_1^2)q_2 - DMp_1, \tag{3.1c}$$

$$\dot{q}_2 = -\alpha q_2 + (\beta_2 + A_0 + Br_2^2 + Cr_1^2)p_2 - DMq_1, \tag{3.1d}$$

where the external forcing A_0, the damping coefficient α, and the frequency offset β_i are given by

$$A_0 = a_0/a\epsilon^2, \quad \alpha = a_{0\min}/a\epsilon^2, \tag{3.2a, b}$$

$$\beta_i = (\omega^2 - \omega_i^2)/(2\epsilon^2\omega^2), \tag{3.3}$$

A, B, C, D are constant coefficients, $M = p_1 q_2 - p_2 q_1$, and $r_i^2 = p_i^2 + q_i^2$ for $i = 1$ and 2. We take the small parameter ϵ as

$$\epsilon^2 = \tfrac{1}{2}(\omega_2^2 - \omega_1^2)/\omega^2, \tag{3.4}$$

so that the relation $\beta_1 - \beta_2 = 1$ holds.

A general formulation for evaluating the coefficients of nonlinear terms is given by Umeki & Kambe (1989). We have applied this formulation to the three cases of the experiments of (i) Ciliberto & Gollub (1985, denoted by CG) for (4, 3) and (7, 2) modes in a circular cell, (ii) Karatsu (1988, denoted by K) for (1, 2) and (4, 1) in a circular cell, and (iii) Simonelli & Gollub (1989, denoted by SG) for (2, 3) and (3, 2) modes in a rectangular cell. The normalized values of coefficients A, B, C, D calculated for the three cases are

$$(A, B, C, D) = (1.0, -0.16, 1.2, -7.9) \quad \text{for CG}, \tag{3.5}$$

$$= (-1.0, 41, 5.0, -27) \quad \text{for K}, \tag{3.6}$$

$$= (0.26, 0.26, 0.32, -1.6) \quad \text{for SG}. \tag{3.7}$$

We do not show these computations here; for the details, see Umeki (1989) concerning SG. We have made some corrections to the previous results, so the values (3.5) for CG are different from those of Umeki & Kambe (1989). The dependence of the coefficient values on the physical parameters is as follows. The values for CG are sensitive to the surface tension because the third resonant mode exists in the region of external forcing frequency examined, and the resonance condition is affected largely by the surface tension. Considerable changes of those values occur in the following two cases: when the capillary length λ varies between 0 and 0.28 cm with fixed values of the forcing frequency and other parameters (depth, radius, etc.); and when the forcing frequency varies with other parameters fixed. But the coefficients for the cases of K and SG are not so sensitive to the forcing frequency and the surface tension.

The dynamical system (3.1*a–d*) has five different stationary states. Introducing the notation $\boldsymbol{r} = (\boldsymbol{r}_1, \boldsymbol{r}_2) = (p_1, q_1, p_2, q_2)$, they are expressed as

$\boldsymbol{r} = (\boldsymbol{0}, \boldsymbol{0})$; Quiescent state (Q)

$(\boldsymbol{r}_1, \boldsymbol{0})$: Mode-1 standing-wave state (S1)

$(\boldsymbol{0}, \boldsymbol{r}_2)$: Mode-2 standing-wave state (S2)

$(\boldsymbol{r}_1, \boldsymbol{r}_2)$ with $M = 0$: Mixed standing-wave state (Ma)

$(\boldsymbol{r}_1, \boldsymbol{r}_2)$ with $M \neq 0$: Mixed standing-wave state (Mb).

The quiescent state is stable (or unstable) if $A_0 \leqslant (or >) (\beta_i^2 + \alpha^2)^{\frac{1}{2}}$. The curve given by

$$A_0 = (\beta_i^2 + \alpha^2)^{\frac{1}{2}} \tag{3.8}$$

in the (f_0, a_0) diagram is a bifurcation curve from a quiescent state to a mode-i standing-wave state, where the driving frequency $f_0 = \Omega/2\pi$ is used for comparison with experiments. The point where two curves (3.8) for $i = 1$ and 2 intersect is named the X point and the frequency and the amplitude at this point X are specified by a subscript asterisk as f_*.

The component of the mode-i standing-wave for $A_i < 0$ (A_i being defined by (2.13)) is given by

$$r_{i\pm} = (p_{i\pm}, q_{i\pm})$$

$$= \left(\left[\frac{\alpha^2+(A_0+\beta_i)[-A_0\pm(A_0^2-\alpha^2)^{\frac{1}{2}}]}{2A_0A_i}\right]^{\frac{1}{2}}, \left[\frac{-\alpha^2+(A_0-\beta_i)[A_0\pm(A_0^2-\alpha^2)^{\frac{1}{2}}]}{2A_0A_i}\right]^{\frac{1}{2}}\right). \quad (3.9)$$

For $A_i > 0$, the plus and minus signs in the right-hand side of (3.9) are inverted.

Mixed standing-wave states (i.e. fixed points of (3.1*a–d*) with all non-zero components) can be shown to satisfy one of the two relations

$$\Delta\beta+(A-C)\,r_1^2+(C-B)\,r_2^2=0, \quad (3.10)$$

$$\beta_1+\beta_2+(A+C+D)\,r_1^2+(B+C+D)\,r_2^2=0, \quad (3.11)$$

where $\Delta\beta = \beta_1-\beta_2\,(=1)$. Stationary states satisfying (3.10) and (3.11) are named Ma and Mb, respectively. The two states satisfying the condition (3.10) are distinguished by a subscript $\pm$. The Ma state yields the relation

$$M = p_1q_2-p_2q_1 = 0. \quad (3.12)$$

The $\mathrm{Ma}_\pm$ state is given by

$$p_{1\pm}^2 = \frac{C\beta_2-B\beta_1}{2(AB-C^2)}\pm\left\{\frac{B-C}{2(AB-C^2)}-\frac{1}{2A_0}\right\}(A_0^2-\alpha^2)^{\frac{1}{2}}, \quad (3.13a)$$

$$q_{1\pm}^2 = \frac{C\beta_2-B\beta_1}{2(AB-C^2)}\pm\left\{\frac{B-C}{2(AB-C^2)}+\frac{1}{2A_0}\right\}(A_0^2-\alpha^2)^{\frac{1}{2}}, \quad (3.13b)$$

$$p_{2\pm}^2 = \frac{C\beta_1-A\beta_2}{2(AB-C^2)}\pm\left\{\frac{A-C}{2(AB-C^2)}-\frac{1}{2A_0}\right\}(A_0^2-\alpha^2)^{\frac{1}{2}}, \quad (3.13c)$$

$$q_{2\pm}^2 = \frac{C\beta_1-A\beta_2}{2(AB-C^2)}\pm\left\{\frac{A-C}{2(AB-C^2)}+\frac{1}{2A_0}\right\}(A_0^2-\alpha^2)^{\frac{1}{2}}. \quad (3.13d)$$

The regions of Ma_+ or Ma_- are restricted in the parameter space (f_0, a_0) given by the condition that the right-hand sides of (3.13*a–d*) are all positive.

For the coefficients (3.6) of K, these regions are

$$(A_0^2-\alpha^2)^{\frac{1}{2}}+\frac{C}{C-B}-\frac{AB-C^2}{(C-B)A_0}(A_0^2-\alpha^2)^{\frac{1}{2}} < \beta_1 < (A_0^2-\alpha^2)^{\frac{1}{2}}$$

$$-\frac{A}{C-A}-\frac{AB-C^2}{(C-A)A_0}(A_0^2-\alpha^2)^{\frac{1}{2}} \quad (3.14a)$$

for Ma_+, and

$$-(A_0^2-\alpha^2)^{\frac{1}{2}}+\frac{C}{C-B}-\frac{AB-C^2}{(C-B)A_0}(A_0^2-\alpha^2)^{\frac{1}{2}} < \beta_1 < -(A_0^2-\alpha^2)^{\frac{1}{2}}$$

$$-\frac{A}{C-A}-\frac{AB-C^2}{(C-A)A_0}(A_0^2-\alpha^2)^{\frac{1}{2}} \quad (3.14b)$$

for Ma_-.

For the coefficients (3.5) of CG and (3.7) of SG, these regions are

$$\beta_1 < (A_0^2-\alpha^2)^{\frac{1}{2}}-\frac{A}{C-A}+\frac{AB-C^2}{(C-A)A_0}(A_0^2-\alpha^2)^{\frac{1}{2}} \quad (3.15a)$$

for Ma_+, and

$$\beta_1 < -(A_0^2-\alpha^2)^{\frac{1}{2}} - \frac{A}{C-A} + \frac{AB-C^2}{(C-A)A_0}(A_0^2-\alpha^2)^{\frac{1}{2}} \tag{3.15b}$$

for Ma_-.

In every case, the regions corresponding to the Ma state are located far from the point X. Since these parameter regions are out of the range of experimental investigations for (3.5) and (3.7) or confined to a small region for (3.6), the Ma state is less important.

The stationary state Mb is given by solving the following equation with (3.10):

$$A_0^2 = \frac{\alpha^2\{\beta_1+\beta_2+(A+C)r_1^2+(B+C)r_2^2\}^2+\{2\alpha^2+\frac{1}{2}UV\}^2}{4\alpha^2+U^2}, \tag{3.16}$$

where

$$U = \Delta\beta+(A-C)r_1^2+(C-B)r_2^2,$$

$$V = \Delta\beta+(A-C-D)r_1^2+(C+D-B)r_2^2.$$

The bifurcation curves of Mb from the states of S1 and S2, are given by

$$A_0 = A_{01}(\beta_1) \equiv \left[\alpha^2+\left\{\frac{-B\beta_1+(C+D)\beta_2}{B+C+D}\right\}^2\right]^{\frac{1}{2}} \tag{3.17}$$

and

$$A_0 = A_{02}(\beta_1) \equiv \left[\alpha^2+\left\{\frac{-A\beta_2+(C+D)\beta_1}{A+C+D}\right\}^2\right]^{\frac{1}{2}}. \tag{3.18}$$

We have examined the stability of the Mb stationary state by solving the quartic equation with respect to the eigenvalue σ of a small perturbation of the form $(\tilde{p}_1, \tilde{q}_1, \tilde{p}_2, \tilde{q}_2)\exp(\sigma\tau)$. It is found that there exists a parameter region near the point X where the Mb state is unstable and Hopf bifurcation occurs; moreover that the numerical integration yields non-periodic behaviour of mode competition between mode 1 and mode 2. We consider further details of the comparison with the three experiments in the next section.

4. Comparison with experimental observations

The system of nonlinear evolution equations developed in §3 is investigated here in detail for the three cases of the nonlinear coefficients (3.5)–(3.7), corresponding to experiments, and the results of numerical analysis are compared to the observations. Each experiment is first reviewed briefly.

4.1. *Interaction between* (4, 3) *and* (7, 2) *modes*

4.1.1. *Experiment*

In the experiment of Ciliberto & Gollub (1985), the fluid cell was mounted on the cone of a loudspeaker in a way that allows vertical forcing with an amplitude of 0–200 μm. The fluid layer was about 1 cm deep in a cylindrical vessel of interior radius $R = 6.35$ cm. The driving frequency is derived from a synthesizer (and a power amplifier). The surface deformation was studied optically by a parallel expanded laser beam passing vertically through the cell. The image formed on a translucent screen located 6 cm above the fluid surface was recorded on videotape and digitized.

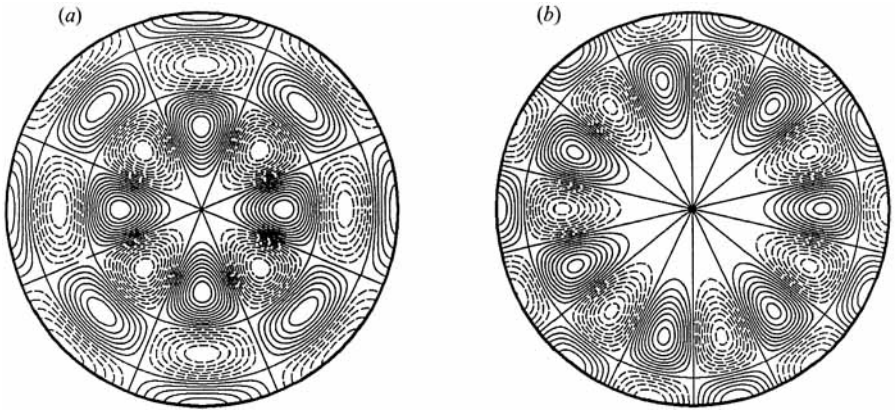

FIGURE 2. Surface mode contours $\psi_n(r,\theta) = \text{const}$: (*a*) $n = (4,3)$ and (*b*) $n = (7,2)$.

From weakly nonlinear theory, the surface displacement is written as a superposition of excited modes as (2.2) and (2.6). In the present case, we have

$$\psi_n(r,\theta) = J_l(\kappa_{lm})\cos(l\theta+\phi_{lm}), \tag{4.1a}$$

$$\eta_n(t) = p_n\cos\omega t + q_n\sin\omega t + (\text{small harmonic terms}), \tag{4.1b}$$

the mode n being denoted as (l,m).

In general the angular phase ϕ_{lm} may be time dependent, but for the phenomenon in the circular cylinder described here, the phase was observed to be time independent. This is consistent with the property of no mode rotation described in §2. A mode develops a parametric instability when the corresponding eigenfrequency is approximately in resonance with one half of the driving frequency $f_0 = \Omega/2\pi$. This leads to a standing wave oscillating at the subharmonic frequency $\frac{1}{2}f_0$. When the mode excitation is not single, there is a slow modulation of the mode amplitudes, and each amplitude is written as (4.1*b*) with the slowly varying envelops p_n and q_n.

The behaviour of the system was plotted in a phase diagram of the driving frequency f_0 and amplitude a_0. A region near the mode competition between (4, 3) and (7, 2) modes was studied in detail. Each surface mode pattern is shown in figure 2, and the phase diagram together with the results of the analysis is given in figure 3. The driving frequency was about 16 Hz. Above the stability boundaries a surface wave oscillating at half the driving frequency is excited in a single stable mode, whereas below them a surface wave is not excited. The shaded area is the region of mode interaction, in which the wave can be described as a superposition of the (4, 3) and (7, 2) modes. The mode amplitudes have a slowly varying envelope with the variations being either periodic or chaotic.

4.1.2. *Results of analysis*

According to the specific values of (3.5), we have $A+C+D<0$ and $B+C+D<0$, therefore the region including Mb is given by $f_0 > f_*$ and $A_{01} < A_0 < A_{02}$. This is consistent with the observation that the periodic and chaotic mode competitions occur in the region $f_0 > f_*$ of the diagram in figure 3. Figure 4 shows a bifurcation diagram which is obtained by plotting the value $M = p_1q_2 - p_2q_1$ at $\dot{q}_2 = 0$ for the driving amplitude a_0 with a fixed frequency $f_0 = 16.05$ Hz. The dynamical equations (3.1*a–d*) are solved numerically using the fourth-order Runge–Kutta scheme. There exist periodic windows between chaotic orbits, which are observed in the experiment

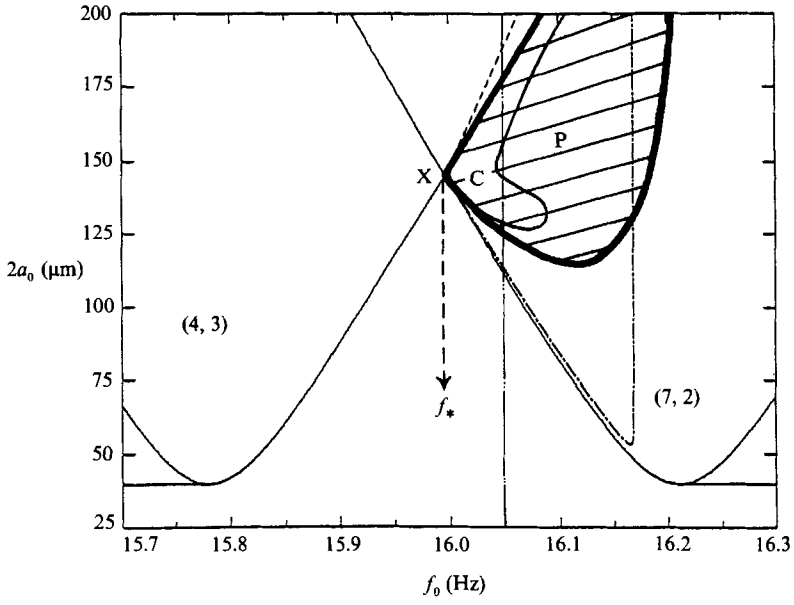

FIGURE 3. Stability diagram in the $(f_0, 2a_0)$-plane for the CG case. Observed and predicted stability boundaries are denoted by thick and thin curves respectively. Periodic and chaotic mode interactions are predicted to occur in a region between the dashed curve and the dashed-dotted curve given by equations (3.17) and (3.18).

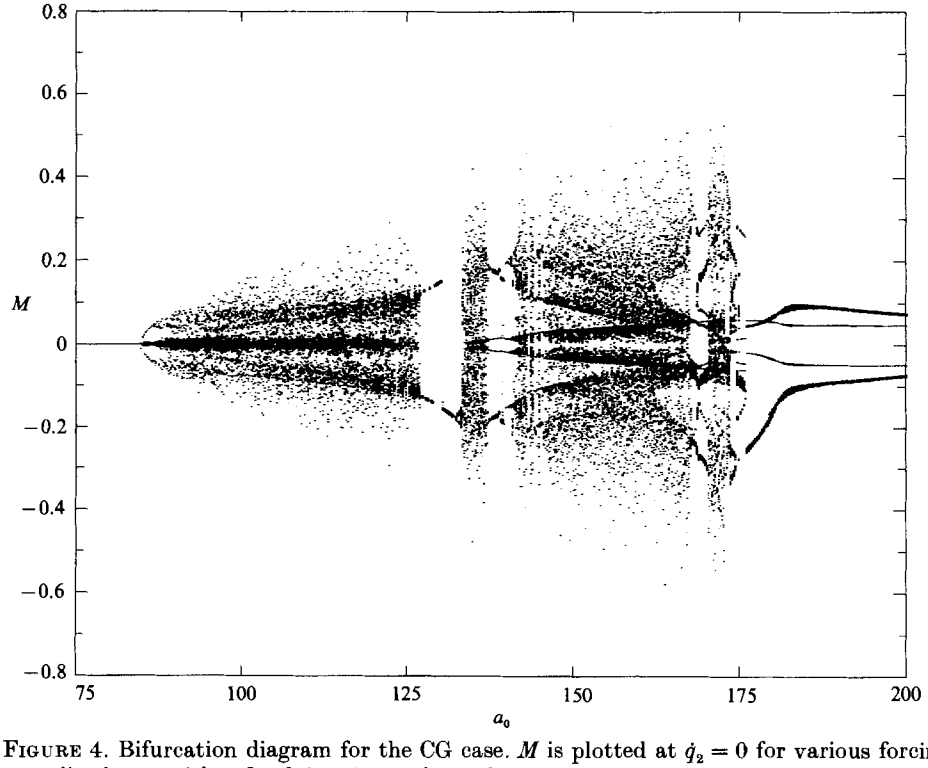

FIGURE 4. Bifurcation diagram for the CG case. M is plotted at $\dot{q}_2 = 0$ for various forcing amplitudes a_0 with a fixed $f_0 = 16.05$ shown by a dashed-dotted-dotted line in figure 3.

of CG. The frequency f_0 lies in a section in which non-periodic behaviour is expected to occur by the theory. In the diagram we can see the bifurcation to chaotic behaviour and periodic windows. Satisfactory agreement has been obtained between the theoretical analysis and the experiment in this case.

4.2. *Interaction between* (1, 2) *and* (4, 1) *modes*

4.2.1. *Experiment*

An experiment on a fluid layer at a moderate depth was carried out by Karatsu (1988),† using an electromagnetic driving mechanism that had more power than a loudspeaker. A circular-cylindrical container of radius $R = 7.2$ cm, filled with water of depth $d = 5.5$ cm, is oscillated vertically with an amplitude of 0.05–2.0 mm. The driving frequency is derived from a synthesizer. The surface oscillation was measured by a wave meter (wire gauge), and the signals are recorded digitally at a sampling time of 20 ms.

In this experiment, a new mode pair of resonant interaction has been found. The modes are excited as a subharmonic resonance of half the driving frequency of about 8.8 Hz, and are expressed as (1, 2) and (4, 1). The driving amplitude was monitored by a capacity sensor.

Figure 5 shows the surface wave patterns of the (1, 2) and (4, 1) modes. The observed phase diagram in the plane of the driving frequency and amplitude is illustrated in figure 6, together with the linear stability curves without damping. Since the difference between the two eigenfrequencies is very small (about 0.2%) for this pair, the experimental stability boundaries for each mode are almost overlapping and indistinguishable. This is in quite a contrast to the previous case of §4.1. The region marked as (1, 2) (or (4, 1)) shows where the single mode (1, 2) (or (4, 1)) is excited. The shaded areas are the regions of mode interaction, which occur on the left side of a vertical symmetry line of the stability curve, as compared with those for the (4, 3) and (7, 2) modes which appear on the right side. In this case too the mode amplitudes have an envelope which varies either periodically or chaotically.

The vertical displacement of the surface was observed at two fixed stations located symmetrically with respect to the centre (180° separation with the same radial position). The signal from each station was recorded digitally at a sampling time of 20 ms. The Fourier spectrum for the single-mode excitation has discrete peaks at the fundamental frequency $\frac{1}{2}f_0$ and its higher harmonics (figure 7*a*). The periodic alternation of the two surface modes is characterized by a spectrum with a peak at a lower frequency in addition to the fundamental and by their interaction peaks. In the chaotic alternation, the spectrum peaks become broad and tend to be continuous. Especially notable is the excitation of a continuous spectrum at low frequencies (figure 7*b*).

The surface displacement in the state of two-mode excitation may be represented as

$$\eta(t, r, \theta) = R_1(t)\, J_1(\kappa_{12} r) \cos(\theta + \phi_1) + R_2(t)\, J_4(\kappa_{41} r) \cos(4\theta + \phi_2) + (\text{small correction terms}). \quad (4.2)$$

It can reasonably be assumed (as mentioned before) that the phases ϕ_1 and ϕ_2 are constant. Denoting the two measuring stations by $r = r_0$ and $\theta = 0, \pi$, we have the wave heights

$$\eta_1(t, r_0, 0) = B_1(t) + B_2(t), \quad (4.3a)$$

$$\eta_2(t, r_0, \pi) = -B_1(t) + B_2(t), \quad (4.3b)$$

† This work is described here at some length because the first report was written in Japanese.

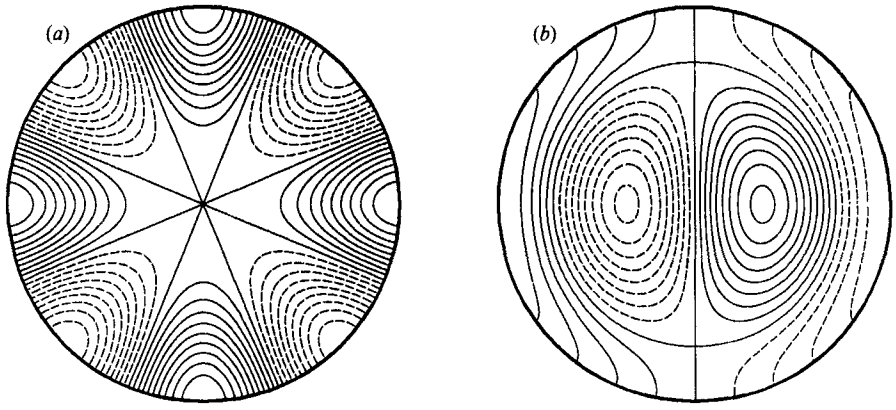

FIGURE 5. Surface mode contours $\psi_n(r,\theta) = \text{const}$: (a) $n = (4,1)$ and (b) $n = (1,2)$.

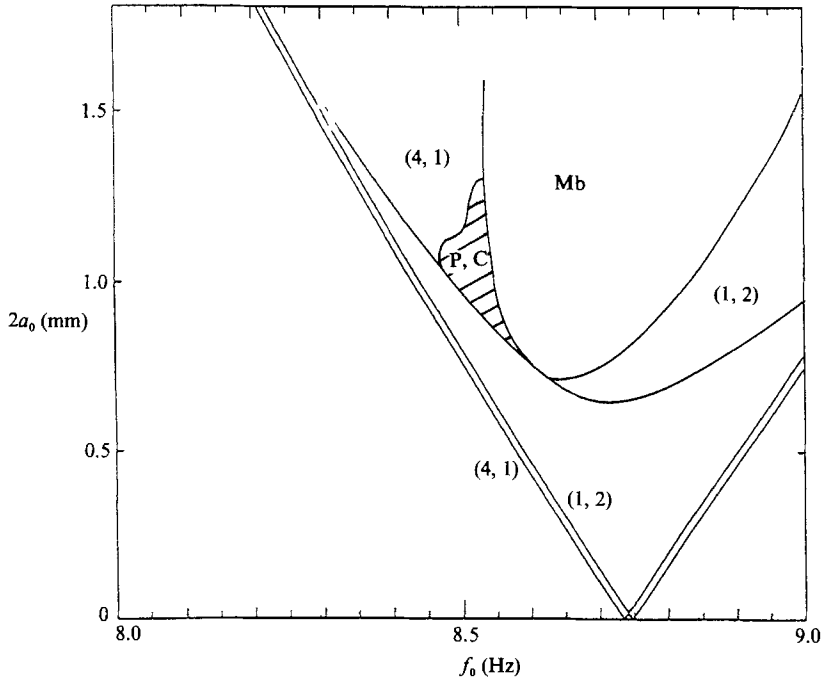

FIGURE 6. Observed phase diagram in the $(f_0, 2a_0)$-plane, together with stability boundaries of the linear theory. In the region denoted as P, C periodic or chaotic interactions are observed.

where $$B_1(t) = R_1 J_1(\kappa_{12} r_0)\cos\phi_1, \quad B_2(t) = R_2 J_4(\kappa_{41} r_0)\cos\phi_2.$$

Therefore, the amplitude of each mode is obtained by addition or subtraction of the signals from the two stations:

$$B_1(t) = \tfrac{1}{2}(\eta_1 - \eta_2), \quad B_2 = \tfrac{1}{2}(\eta_1 + \eta_2). \tag{4.4a, b}$$

In this way, mode excitation has been recorded. Figure 8 illustrates three cases of mode amplitudes from the data sampled at every 20 ms for five minutes and shown in terms of the period $T = 1/f_0$ of the driving oscillation: (a) a single-mode excitation of (1, 2), (b) a nearly periodic alternation, and (c) a chaotic mode competition.

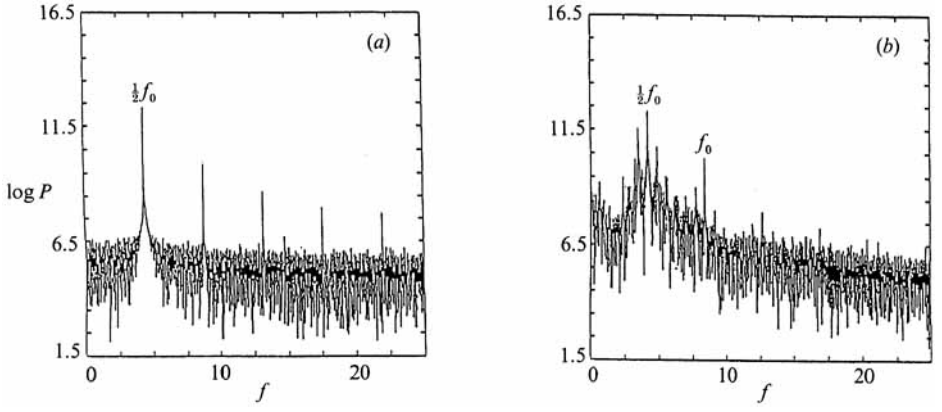

FIGURE 7. Fourier spectrum of the signals at a fixed station. (*a*) Single-mode excitation and (*b*) chaotic mode alternation.

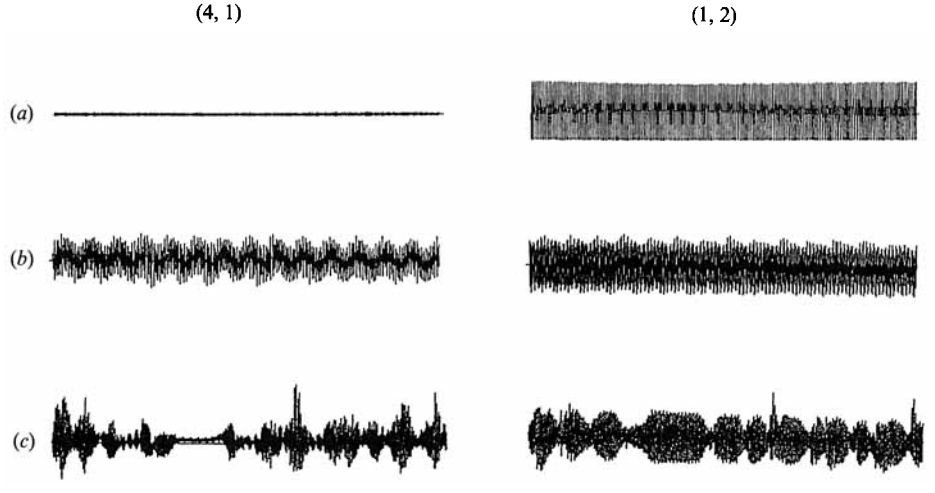

FIGURE 8. Mode amplitudes over a five minute period: (*a*) single-mode excitation of the (1, 2) mode; (*b*) nearly periodic alternation and (*c*) chaotic mode competition.

4.2.2. *Results of analysis*

From the coefficient values of (3.6), we have inequalities $A+C+D<0$ and $B+C+D>0$ for this case, and the region including Mb is given by $\beta_1 \geqslant 0.5$, $A_0 > A_{01}$ and $\beta_1 < 0.5$, $A_0 > A_{02}$. Figure 9 shows the parameter-space diagram (where the difference of two eigenfrequencies is taken to be larger than the value calculated by linear theory). The parameter-space regions where S2 and Mb were found in the experiment (figure 6) coincide with the result of the theoretical analysis (figure 9) based on the coefficients (3.6). However, the regions of periodic and chaotic mode competition do not coincide. In this respect it should be noted that ratio of the wave amplitude to the wavelength in the experimental case of mode competition is of order unity, not small at all, implying that nonlinearity is too strong. Therefore higher-order nonlinear terms will be required to account for the discrepancy not only in the Hamiltonian but also in the damping effect. The observed S1 region on the left side is not predicted either. Thus the prediction by the third-order evolution equations is not so satisfactory in this case.

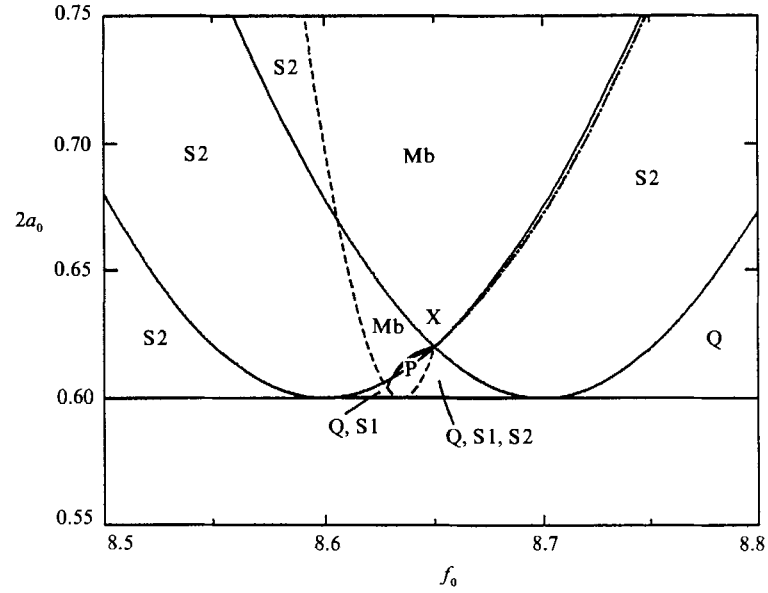

FIGURE 9. Predicted stability diagram for the K case. The lettering in each region refers to the stable state. A periodic mode competition is confined to a small region P near the point X.

4.3. *Interactions in quadrilateral cells*

4.3.1. *Experiment*

In a square cell, two surface modes that transform into each other under a 90° spatial rotation have a degenerate eigenfrequency. This degeneracy is broken in a rectangular cell. The effect of detuning of two resonant modes in these geometries has been investigated by Simonelli & Gollub (1989). Such a degeneracy of the surface waves exists in a circular cylinder too, i.e. there are modes which transform into each other under a spatial rotation. However, no attempt has been made so far to investigate the effect of detuning by making the cross-section, say, elliptic. Resonant interactions of two nearly degenerate modes which were studied in the circular cylinder are concerned with modes having different wavenumbers both in the radial and angular coordinates.

The experiments by Simonelli & Gollub were performed in a square cell of size 6.17 by 6.17 cm and a rectangular cell of size 6.17 by 6.6 cm, with a depth of 2.5 cm. The vertical oscillation was provided by an electromagnetic shaker driven by a synthesizer. The driving amplitude (more directly, vertical acceleration) was measured with an accelerometer. In this experiment, the stability boundaries were determined in an automated fashion as a function of driving amplitude a_0 and frequency f_0. The surface deformation of each spatial mode in a general rectangular geometry has the form

$$Z_{mn}(t,x,y) = [A_{mn}(t)\cos\omega t + B_{mn}(t)\sin\omega t]\cos\frac{m\pi x}{L_x}\cos\frac{n\pi y}{L_y}, \tag{4.5}$$

where $\omega = \pi f_0$, m and n are integers, and L_x and L_y are horizontal dimensions of the cell in the x- and y-directions. The coefficients A_{mn} and B_{mn} are the in-phase and out-of-phase amplitudes (with respect to the driving phase) that vary on a timescale much larger than $1/\omega$. The mode Z_{mn} is denoted as (m, n). Detailed observations were performed on the mode pair (3, 2) and (2, 3).

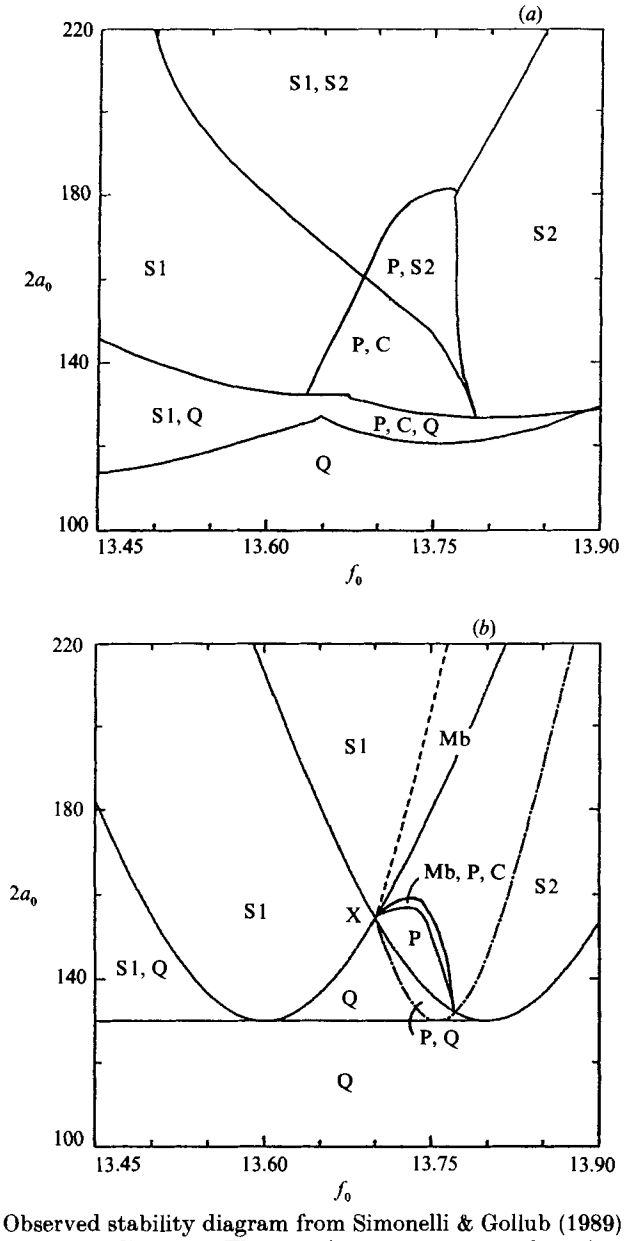

FIGURE 10. (*a*) Observed stability diagram from Simonelli & Gollub (1989). (*b*) Predicted stability diagram for the corresponding case. The complex structure near the point X is caused by the fact that Hopf bifurcation from the Mb state is subcritical.

In the completely degenerate case (square cell), three primary regions have been identified in the parameter space of f_0 and a_0: flat state, mixed state and pure state (owing to the symmetry, either pure state can be found depending on the initial conditions). There are also intermediate regions between those states, characterized by the coexistence of two of them. However, no alternation of amplitudes between the two degenerate modes has been observed. Thus the x–y symmetry of the fluid cell yields no competitive interaction between two resonant modes.

The effect of removing the degeneracy was investigated with a rectangular cell.

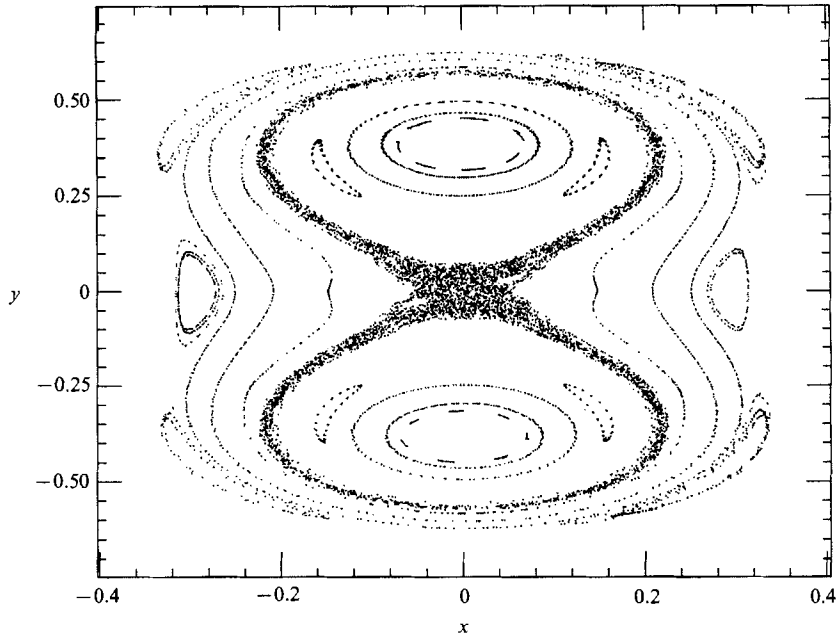

FIGURE 11. Poincaré map of the equations (5.3) on the plane $(x, y) = ((2P_1)^{\frac{1}{2}}\cos Q_1, (2P_1)^{\frac{1}{2}}\sin Q_1)$ at $Q_2 = 0$, showing homoclinic chaos. Initial values are $P_2 = 0.25$, $Q_2 = 0$, $P_1 = 0.001$, 0.05 and $Q_1 = 2\pi k/40$ $(k = 1, \ldots, 40)$.

The aspect ratio $6.6/6.17 \approx 1.07$, different from 1, produces a difference of about 1.5% between the resonant frequencies of the two modes (3, 2) and (2, 3). Four primary regions are identified in the parameter space: flat state; pure (3, 2) state; pure (2, 3) state; and the state of periodic or chaotic time dependence. There are also intermediate regions between those states. The last time-dependent state is the consequence of symmetry breaking of the container geometry.

4.3.2. *Results of analysis*

From the coefficients (3.7) for the rectangular cell, we have $A+C+D = B+C+D < 0$ and the region including Mb is given by $\beta_1 \geqslant 0.5$ and $A_{01} < A_0 < A_{02}$. The parameter-space diagram from the theory is shown in figure 10(*b*) and is compared to that of the experiment in figure 10(*a*). Topological coincidence in the diagram between experimental and theoretical results is obtained. The only difference is that there exists a stable Mb state in the analytical result, but it is not found in the experiment. The parameter region where the Mb state is stable in (*b*) is replaced by the coexistence of the S1 and S2 states in (*a*). It might be an effect of nonlinearity of higher orders, or due to the smallness of the one-mode amplitude of the Mb state, that the mixed state is not observed.

5. Homoclinic chaos in an averaged Hamiltonian system

We consider here homoclinic chaos of our dynamical system. It has been shown numerically by Umeki (1989) that the Hamiltonian system (2.14) for suitable parameters without damping ($\alpha = 0$) and forcing ($a_0 = 0$) has homoclinic orbits, and that when a small forcing is added, homoclinic orbits start to have transverse

intersections. This is similar to the mathmatical work of Holmes (1986) on the 1:2:2 resonance but different with respect to the nonlinearity: it is second-order in Holmes' analysis but third-order in ours. This difference comes from the internal–external resonance conditions.

We perform the following canonical transform to the dynamical system (3.1*a–d*):

$$(q_i, p_i) = ([2\tilde{P}_i]^{\frac{1}{2}} \cos \tilde{Q}_i, [2\tilde{P}_i]^{\frac{1}{2}} \sin \tilde{Q}_i), \tag{5.1}$$

and perform a further canonical transformation,

$$\tilde{Q}_1 = Q_1 + Q_2, \quad \tilde{Q}_2 = Q_2, \quad \tilde{P}_2 = P_2 - P_1, \quad \tilde{P}_1 = P_1. \tag{5.2}$$

Then the system is expressed as

$$\dot{P}_1 = -2DP_1(P_2 - P_1) \sin 2Q_1 - 2A_0 P_1 \sin 2(Q_1 + Q_2) - 2\alpha P_1, \tag{5.3a}$$

$$Q_1 = \Delta\beta + EP_1 + FP_2 - D(P_2 - 2P_1) \cos 2Q_1 - A_0[\cos 2(Q_1 + Q_2) - \cos 2Q_2], \tag{5.3b}$$

$$\dot{P}_2 = -2A_0[P_1 \sin 2(Q_1 + Q_2) + (P_2 - P_1) \sin 2Q_2] - 2\alpha P_2, \tag{5.3c}$$

$$\dot{Q}_2 = \beta_2 + 2BP_2 + FP_1 - DP_1 \cos 2Q_1 - A_0 \cos 2Q_2, \tag{5.3d}$$

where $$E = 2(A + B - 2C - D), \quad F = 2(C - B) + D.$$

Using the reduction method (Guckenheimer & Holmes 1983), we consider the Poincaré section on the plane $Q_2 = \text{const.}$ with $\alpha = 0$ (a conservative Hamiltonian system). The parameters A, B, C, D, β_1, β_2 are taken as

$$A = B = C = -3, \quad D = -4, \quad \beta_1 = 0, \quad \beta_2 = -1. \tag{5.4}$$

The assumptions for the reduction method are (i) existence of a homoclinic orbit when $a_0 = 0$ and (ii) $\dot{Q}_2 \neq 0$ on and in a neighbourhood of the homoclinic orbit. We choose the parameters so as to satisfy these assumptions. One of the results of our numerical analysis are shown in figure 11 for various initial conditions. We observe stochastic layers near the homoclinic orbit in the form of figure 8 in addition to several invariant manifolds.

When a small damping is added, the assumption (ii) does not hold. This is inevitable because the orbit tends to an attractor, which may be a fixed point (or a periodic orbit, or a strange attractor). The type of the attractor should be determined by a bifurcation analysis. In the above case it is a fixed point. The assumption $\dot{Q}_2 \neq 0$ does not hold in the attractors for many sets of the parameters.

This result implies that the non-periodic mode competition observed in the experiments occurs in strongly dissipative systems and is quite different from the homoclinic chaos as considered by Holmes (1986). Therefore we have to distinguish the two kinds of chaotic motion.

6. Summary

Based on Miles' formulation, a system of nonlinear evolution equations is derived as an averaged system for parametric excitation of surface waves under vertical forcing of amplitude a_0, the forcing frequency f_0 being chosen at near twice the frequencies of two nearly degenerate internal modes. The results of the analysis are presented in a unified fashion and compared with three experimental observations. The system of evolution equations for four variables is derived from an averaged Hamiltonian (two degrees of freedom) except for damping terms, and includes three kinds of linear terms which are characterized by a damping constant α, a forcing

amplitude a_0 and frequency offset β_i ($i = 1, 2$; corresponding to two internal resonant modes). The nonlinearity of the differential equations is of third order and described by four constant coefficients which are all different for the three experimental cases.

As a fourth case, the Hamiltonian system without damping has been studied. The two-degrees-of-freedom system in the absence of external forcing has a homoclinic orbit, which is disrupted into a stochastic layer under a small external perturbation.

The dynamical system of differential equations has five different stationary states: a quiescent state, two single-mode standing-wave states and two mixed-mode states. Further, there exist regions in the parameter space (f_0, a_0) in which all of the stationary states are unstable. In those regions, numerical integration has been performed, and time-dependent states have been found, which represent periodic or non-periodic (chaotic) behaviour of mode competition between the two internally resonant modes.

Concerning the comparison with the three observations, the analytical results for a pair of (4, 3) and (7, 2) modes in a circular cell are in satisfactory agreement with the experiment by Ciliberto & Gollub, and the results for the (2, 3) and (3, 2) mode pair in a rectangular cell are also in good agreement with the experiment by Simonelli & Gollub, except for presence/absence of mixed-mode excitation. However, for the (1, 2) and (4, 1) mode pair in a circular cell, the agreement is only modest, and in particular the time-dependent motions of the numerical integration are in a different place from the observation by Karatsu. This implies that nonlinearity of higher orders should be taken into consideration to account for the observed time-dependent state of chaotic mode interaction.

The chaotic mode competition observed in the experiments is considered to be relevant to the homoclinic chaos of the Hamiltonian system of two degrees of freedom studied by Holmes (1986). However, the present analysis is counter to that view, and shows that the orbit tends to a point attractor, not to a chaotic attractor, when a damping is added. The chaotic mode competition observed in the experiments occurs in a strongly dissipative system, and is considered to be a quite different phenomenon from the homoclinic chaos of the present Hamiltonian system.

One of the authors (T. K.) remembers the pleasant days fifteen years ago when he stayed at Cambridge for sixteen months and spent with George Batchelor. This happy memory is always encouraging him during his study of fluid mechanics afterwards.

REFERENCES

Benjamin, T. B. & Ursell, F. 1954 The stability of the plane free surface of a liquid in vertical periodic motion. *Proc. R. Soc. Lond.* A **225**, 505–515.

Ciliberto, S. & Gollub, J. P. 1984 Pattern competition leads to chaos. *Phys. Rev. Lett.* **52**, 922–925.

Ciliberto, S. & Gollub, J. P. 1985 Chaotic mode competition in parametrically forced surface waves. *J. Fluid Mech.* **158**, 381–398.

Crawford, J. D., Knobloch, E. & Riecke, H. 1988 Mode interactions and symmetry. In *Proc. Intl Conf. on Singular Behavior and Nonlinear Dynamics*. World Scientific, preprint.

Faraday, M. 1831 On the forms and states assumed by fluids in contact with vibrating elastic surfaces. *Phil. Trans. R. Soc. Lond.* **121**, 319–340.

Feng, Z. C. & Sethna, P. R. 1989 Symmetry-breaking bifurcations in resonant surface waves. *J. Fluid Mech.* **199**, 495–518.

Funakoshi, M. & Inoué, S. 1988 Surface waves due to resonant horizontal oscillation. *J. Fluid Mech.* **192**, 219–247.

GOLLUB, J. P. & MEYER, C. W. 1983 Symmetry breaking instabilities on a fluid surface. *Physica* **6D**, 337–346.

GU, X. M. & SETHNA, P. R. 1987 Resonant surface waves and chaotic phenomena. *J. Fluid Mech.* **183**, 543–565.

GUCKENHEIMER, J. & HOLMES, P. J. 1983 *Nonlinear Oscillations, Dynamical Systems and Bifurcations of Vector Fields*, §4.8. Springer.

HOLMES, P. 1986 Chaotic motions in a weakly nonlinear model for surface waves. *J. Fluid Mech.* **162**, 365–388.

KARATSU, M. 1988 Nonlinear resonance and chaos of surface waves of water. Master thesis, University of Tokyo (in Japanese).

KEOLIAN, R. & RUDNICK, I. 1984 The role of phase locking in quasi-periodic surface waves on liquid helium and water. *Proc. Intl Sch. Phys. Frontiers in Physical Acoustics* (ed. D. Sette), pp. 189–199. North-Holland.

KEOLIAN, R., TURKEVICH, L. A., PUTTERMAN, S. J., RUDNICK, I. & RUDNICK, J. A. 1981 Subharmonic sequences in the Faraday experiment: departure from period doubling. *Phys. Rev. Lett.* **47**, 1133–1136.

MERON, E. & PROCACCIA, I. 1986*a* Low dimensional chaos in surface waves: Theoretical analysis of an experiment. *Phys. Rev.* A **34**, 3221–3237.

MERON, E. & PROCACCIA, I. 1986*b* Theory of chaos in surface waves: the reduction from hydrodynamics to few-dimensional dynamics. *Phys. Rev. Lett.* **56**, 1323–1326.

MILES, J. W. 1976 Nonlinear surface waves in closed basins. *J. Fluid Mech.* **75**, 419–448.

MILES, J. W. 1984*a* Resonant motion of a spherical pendulum. *Physica* **11D**, 309–323.

MILES, J. W. 1984*b* Resonantly forced gravity waves in a circular cylinder. *J. Fluid Mech.* **149**, 15–31.

MILES, J. W. 1984*c* Nonlinear Faraday resonance. *J. Fluid Mech.* **146**, 285–302.

MILES, J. W. 1984*d* Resonant non-planer motion of a stretched string. *J. Acoust. Soc. Am.* **75**, 1505–1510.

MILES, J. W. 1988 A note on nonlinear Faraday resonance (preprint).

NAGATA, M. 1989 Nonlinear Faraday resonance in a box with a square base. *J. Fluid Mech.* **209**, 265–284.

NAYFEH, A. H. 1987 Surface waves in closed basins under parametric and internal resonances. *Phys. Fluids* **30**, 2976–2983.

RAYLEIGH, LORD 1883 On the crispations of fluid resting on a vibrating support. *Phil. Mag.* **16**, 50–58 (*Scientific Papers*, vol. 2, pp. 212–219).

SIMONELLI, F. & GOLLUB, J. P. 1989 Surface wave mode interactions: effects of symmetry and degeneracy. *J. Fluid Mech.* **199**, 471–494.

UMEKI, M. 1989 Faraday resonance in rectangular geometry (preprint).

UMEKI, M. & KAMBE, T. 1989 Nonlinear dynamics and chaos in parametrically excited surface waves. *J. Phys. Soc. Japan* **58**, 140–154.